Modelling the hydrodynamic characteristics of gas-liquid-solid fluidized bed using Artificial Neural Networks

A Project submitted to the
National Institute of Technology, Rourkela

In partial fulfilment of the requirements
of
Bachelor of Technology (Chemical Engineering)

By

M. Ajay kumar
Roll No. 10600033

Under the guidance of
Dr. H. M. Jena

DEPARTMENT OF CHEMICAL ENGINEERING
NATIONAL INSTITUTE OF TECHNOLOGY, ROURKELA
ORISSA -769 008, INDIA

2010

DEPARTMENT OF CHEMICAL ENGINEERING
NATIONAL INSTITUTE OF TECHNOLOGY,
ROURKELA -769 008, INDIA

CERTIFICATE

This is to certify that the thesis entitled "**Modelling the hydrodynamic chracteristics of gas-liquid-solid fluidized bed using Artificial Neural Networks",** submitted by **M. Ajay Kumar** to National Institute of Technology, Rourkela is a record of bonafide project work under my supervision and is worthy for the partial fulfillment of the degree of Bachelor of Technology (Chemical Engineering) of the Institute. The candidate has fulfilled all prescribed requirements and the thesis, which is based on candidate's own work, has not been submitted elsewhere.

Supervisor
Dr. H. M. Jena
Department of Chemical Engineering
National Institute of Technology
Rourkela,
INDIA.

ACKNOWLEDGEMENT

With a feeling of great pleasure, I express my sincere gratitude to **Dr. H. M. Jena** for his superb guidance, support and constructive criticism, which led to the improvements of this project work.

I am also grateful to **Prof. S. K. Agarwal,** Head of the Department, Chemical Engineering for providing the necessary opportunities for the completion of this project.

M. Ajay Kumar (Roll No.10600033)

4th year

B. Tech.

Department of Chemical Engineering

National Institute of Technology, Rourkela

ABSTRACT

Gas–liquid–solid fluidized beds are used extensively in the refining, petrochemical, pharmaceutical, biotechnology, food and environmental industries. The fundamental characteristics of a three-phase fluidized bed have been recently studied extensively. The reviews indicate the importance of the information of phase holdup and bed voidage characteristics, in the optimal design of a three-phase fluidized bed reactor.

The various hydrodynamic parameters of three phase fluidized bed have been modeled using Artificial Neural Networks (ANNs). ANNs are good at modeling of non linear parameters, with the ability to generalize the relationships among the data. The data for developing the models has been generated using various correlations available from literature. These correlations are valid for different ranges of the variables. So, artificial neural networks are trained using this vast data range and a generalized model for the hydrodynamic parameters is developed.

This project report can be divided mainly into three parts. The first part discusses about importance of gas-liquid-solid fluidized bed, their modes of operation, important hydrodynamic properties those have been studied either related to modeling and applications of gas-liquid-solid fluidized bed. The second part gives an overview of the basics of Artificial Neural Networks (ANNs) and the various architectures of neural networks that are commonly used for modeling. The third part consists of the details of the problem description and the approach used by ANN to model the hydrodynamic characteristics. The results show that the model has been effective in generalizing the relationship of various hydrodynamic characteristics with their respective independent variables.

Kewords: Hydrodynamics; gas-liquid-solid fluidized bed; artificial neural network; bed voidage; gas holdup; liquid holdup.

CONTENTS

LIST OF FIGURES

LIST OF TABLES

NOMENCLATURE

Ut = Terminal liquid velocity (m/s)

U_L = superficial liquid velocity (m/s)

p = Input signal

f = Transfer function

w = Weights

b = Bias constants

R = No. of elements in input vector

s = No. of neurons in input layer

x = Input value

t =Time(s)

n_H =no. of nodes in hidden layer

Re_L =Reynolds no. of liquid

Re_g =Reynolds no. of gas

Fr_g =Froude no. of gas

Fr_L =Froude no. of liquid

W_m=Modified Weber no.

Ca_g=Capillary group

Eo=Eotvos no.

ε = Bed voidage

ε_g= gas holdup

ε_l = liquid holdup

CHAPTER-1

INTRODUCTION

CHAPTER 1

INTRODUCTION

In a typical gas–liquid–solid three-phase fluidized bed, solid particles are fluidized primarily by upward concurrent flow of liquid and gas, with liquid as the continuous phase and gas as dispersed bubbles if the superficial gas velocity is low. Because of the good heat and mass transfer characteristics, three-phase fluidized beds or slurry bulb columns (ut < 0.05 m/s) have gained considerable importance in their application in physical, chemical, petrochemical, electrochemical and biochemical processing (Fan, 1989).

Intensive investigations have been performed on three-phase fluidization over the past few decades; however, there is still a lack of detailed physical understanding and predictive tools for proper design and scale-up of such reactors. The calculation of hydrodynamic parameters in these systems mainly relies on empirical correlations or semi- theoretical models. But these correlations have been quantifies only for specific ranges of variables. So, their use has been limited for practical applications (Kumar, 2009)

Artificial neural networks provide a non-linear mapping between input and output variables and are also useful in providing crosscorrelation among these variables. An ANN consists of a layered network of neurons (nodes), with each neuron connected to a large number of others. The input signal to the network is passed among the neurons, with each neuron calculating its own output using weighting associated with connections. ANNs provide capabilities such as learning, self-organization, generalization and training; and are excellent for trend prediction for processes that are non-linear, poorly-understood, and too complex for accurate mathematical modeling.

The hydrodynamic characteristics, viz. bed expansion, gas holdup and liquid holdup profile of a co-current three-phase fluidized bed have been investigated using the state of the art tools of neural network modeling. The factors affecting the parameters are gas velocity, gas density, liquid velocity, liquid viscosity, particle diameter etc. These factors combined into various dimensionless groups are fed as input to the neural networks for training. The trained neural networks are then used for predicting the hydrodynamic parameters for any new set of inputs. Thus the ANN model has been developed for generalizing the relationship between the variables.

CHAPTER-2

LITERATURE REVIEW

CHAPTER 2

LITERATURE REVIEW

2.1Three phase fluidization.

Gas-liquid-solid fluidization also known as three-phase fluidization is a subject of fundamental research since the last four decades due to its industrial importance. Since then considerable progress has been made with respect to an understanding of the phenomenon of gas-liquid-solid fluidization. The successful design and operation of a gas-liquid-solid fluidized bed system depends on the ability to accurately predict the fundamental properties of the system. Gas-liquid-solid fluidization is defined as an operation in which a bed of solid particles is suspended in gas and liquid media due to the net drag force of the gas and/or liquid flowing opposite to the net gravitational force (or buoyancy force) on the particles. Such an operation generates considerable, intimate contact among the gas, liquid and the solid in the system and provides substantial advantages for application in physical, chemical or biochemical processing involving gas, liquid and solid phases. The state of the gas-liquid-solid fluidization is strongly dependent on the geometry of the bed, methods of gas-liquid injection, and the presence of a retaining grid or internals. This is exemplified by the development and the operation of a tapered fluidized bed, spouted bed, semi fluidized bed and draft tube spouted bed (Jena, 2009)

2.1 Applications of gas-liquid-solid fluidized bed

Gas-liquid-solid fluidized beds have emerged in recent years as one of the most promising devices for three-phase operations. They are of considerable industrial importance because of their wide use for chemical, petrochemical and biochemical processing. As three-phase reactors, they have been employed in hydrogenation and hydro-sulphurization of residual oil for coal liquefaction, in the bio-oxidation process for wastewater treatment, and in turbulent contacting

absorption for flue gas desulphurization. Three-phase fluidized beds are also often used in physical operations.

Fluidized bed units are also found in many plant operations in pharmaceuticals and mineral industries. Fluidized beds serve many purposes in industry, such as facilitating catalytic and non-catalytic reactions, drying and other forms of mass transfer. They are especially useful in the fuel and petroleum industry for things such as hydrocarbon cracking and reforming as well as oxidation of naphthalene to phthalic anhydride (catalytic), or coking of petroleum residues (non-catalytic). Catalytic reactions are carried out in fluidized beds by using a catalyst as the cake in the column, and then introducing the reactants. In catalytic reactions, gas or liquid is passed through a dry catalyst to speed up the reaction (Kumar, 2009)

2.2 Modes of operation of gas-liquid-solid fluidized bed and flow regimes

Gas-liquid-solid fluidization can be classified mainly into four modes of operation. These modes are co-current three-phase fluidization with liquid as the continuous phase (mode I-a); co-current three-phase fluidization with gas as the continuous phase (mode-I-b); inverse three-phase fluidization (mode II-a); and fluidization represented by a turbulent contact absorber (TCA) (mode II-b). Modes II-a and II-b are for a countercurrent flow of gas and liquid. Various methods are possible in evaluating the operating and design parameters for each mode of operation.

Based on the differences in flow directions of gas and liquid and in contacting patterns between the particles and the surrounding gas and liquid, several types of operation for gas-liquid-solid fluidizations are possible. Three-phase fluidization is divided into two types according to the relative direction of the gas and liquid flows, namely, co-current three-phase fluidization and co-current three-phase fluidization (Bhatia and Epstein, 1974). This is shown in fig.2.1.

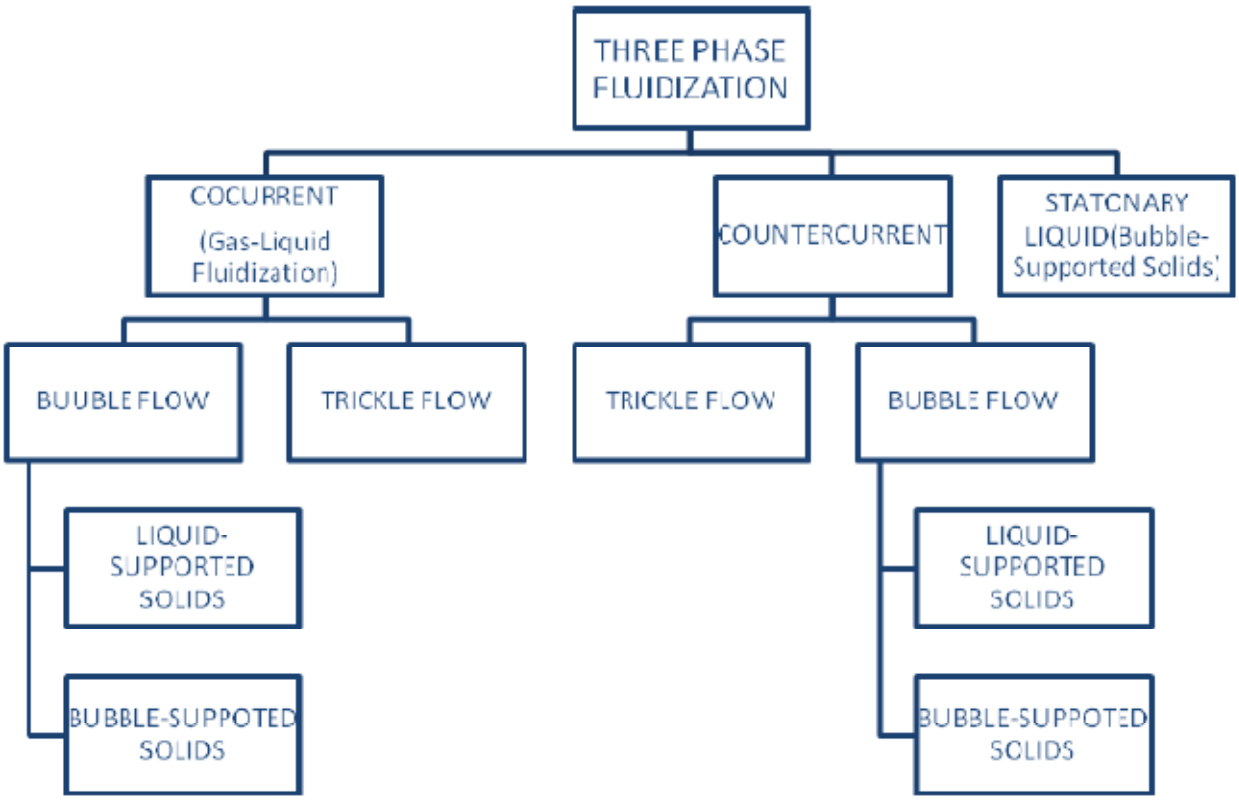

Fig.2.1: Taxonomy of Three-Phase Fluidized Beds as given by Epstein (Kumar, 2009)

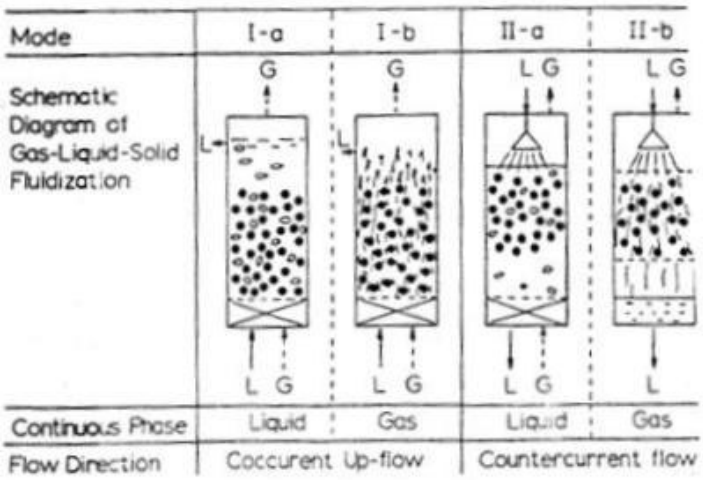

Fig.2.2: Modes of operation of gas-liquid-solid fluidized bed (Kumar, 2009).

In co-current three-phase fluidization, there are two contacting modes characterized different hydrodynamic conditions between the solid particles and the surrounding gas and liquid. These modes are denoted as mode I-a and mode I–b**,** (Fig. 2.2). Mode I-a defines co-current three-phase fluidization with liquid as the continuous phase, while mode I-b defines co-current three-phase fluidization with gas as the continuous phase. In mode I-a fluidization, the liquid with the gas-forming discrete bubbles supports the particles. Mode I-a is generally referred as to as gas-liquid fluidization. Countercurrent three-phase fluidization with liquid as the continuous phase, denoted as mode II-a in fig.2, is known as inverse three-phase fluidization. Countercurrent three-phase fluidization with gas as the continuous phase, denoted as mode II-b in fig.2.2, is known as a turbulent contact absorber, fluidized packing absorber, mobile bed, or turbulent bed contactor. In mode II-a operation the bed of particles with density lower than that of the liquid is fluidized by a downward liquid flow, opposite to the net buoyant force on the particles, while the gas is introduced counter currently to that liquid forming discrete bubbles in the bed. In the mode II-b operation (TCA operation), an irrigated bed of low-density particles is fluidized by the upward flow of gas as a continuous phase. When the bed is in a fully fluidized state, the vigorous moment of wetted particles give rise to excellent gas-liquid contacting. The gas and liquid flow rates in the TCA are much higher than those possible in conventional countercurrent packed beds, since the bed can easily exposed to reduce hydrodynamics resistances (Kumar, 2009).

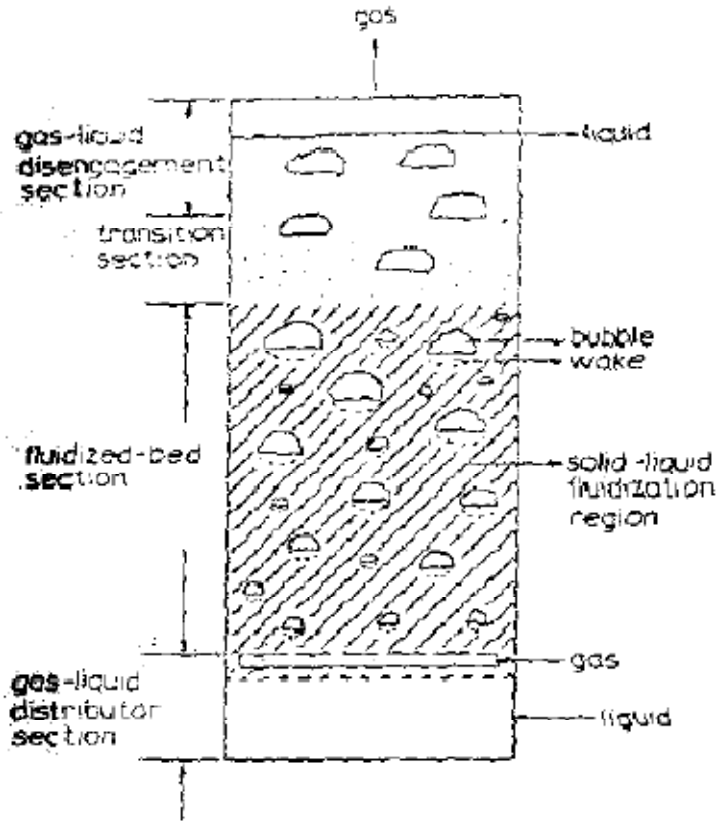

Fig.2.3: Schematic representation of the Mode I-a fluidized bed reactor (Kumar, 2009)

2.3 Important hydrodynamic parameters studied in gas-liquid-solid fluidization

Previously the studies related to three-phase fluidized bed reactors have been directed towards the understanding of the complex hydrodynamics, and its influence on the phase holdup and transport properties. In literature, the hydrodynamic behavior, viz., the pressure drop, minimum fluidization velocity, bed expansion and phase hold-up of a co-current gas–liquid–solid three-phase fluidized bed, were examined using liquid as the continuous phase and gas as the discontinuous phase (Jena et al. 2008). Recent research on fluidized bed reactors focuses on the following topics:

(a) Flow structure quantification: The quantification of flow structure in three-phase fluidized beds mainly focuses on local and globally averaged phase holdups and phase velocities for

different operating conditions and parameters. Lee and DeLasa (1987) investigated bubble phase holdup and velocity in three-phase fluidized beds for various operating conditions using experimental techniques like electro-resistivity probe and optical fiber probe.

(b) Burghardt et al. (2002) studied the hydrodynamics of a three-phase reactor operating at an elevated pressure in the pulsing flow regime. Various parameters were found that characterize the pulsing flow of fluids, namely the velocity of pulses travelling along the bed, the frequency of pulsations and their structure, i.e., the length of the pulses and that of the liquid-rich zone.

2.4 Recent applications of ANN to multiphase fluidization

Multiphase flows in pipes can lead to a large number of different geometric configurations and phase fractions. This obviously poses an intractable problem, because it is difficult to determine a priori which configuration the flow will assume.

Peng et al. proposed a method based on fuzzy logical neural network to recognize oil-gas two-component flow patterns. They first used electrical capacitance tomography (ECT) to monitor the flour main flow patterns inside the pipeline, which were stratified, annular, slug, and bubble flow. For each flow condition, 28 dependent measured capacitance values were obtained using an 8-electrode capacitance transducer and fed into a fuzzy logic module, which converted the input data to fuzzy format and fed the input to a back-propagation feed forward neural network. The output of the network was sent to another module, which used the maximum likelihood criterion and estimated the most likely flow regime. They claimed good agreement was achieved but no quantitative result was given (Xie, 2004)

Sun et al. developed a neural network scheme to identify flow regimes and measure quality in gas-liquid two-phase flow systems using differential pressure signals. Differential pressure

signals were sampled and 20000 data points were acquired at a time. They applied wavelet analyses to the measured differential pressure signals and extracted a feature called scale energy ratio (SER). A three-layer backpropagation neural network was then adopted to map the multi-scale data to the flow regimes they observed, which included annular, bubbly, plug, and slug flow. SER at six different scales were populated to the neural network as inputs. Binary outputs were expected to represent the flow regimes. Their tests showed an acceptable correct identification rate from 81.3% to 90.0% (Xie, 2004)

Otawara et al. developed an artificial neural network model to reveal the dynamic behavior of a three-phase fluidized bed.. An optical transmittance probe was employed to emit a laser beam across the channel and the intensity received by the detector was converted by phototransistor into voltage signals. In the three-phase flow, the particles passage through the laser beam were recognized as spike signals while bubble passages were recognized as broad oscillating signals. An artificial neural network was trained with the superficial gas velocity plus seven time-series data comprising the proceeding and current temporal intervals, In-6, In-5, In-4, In-3, In-2, In-1. Each of them was the time period between two sequential signals representing bubble or particle passage and generated from the optical probe voltage output. The output of the network was the succeeding temporal interval, In+1. Eleven hidden nodes were chosen to avoid overtraining.

CHAPTER-3

ARTIFICIAL NEURAL NETWORK MODELS

CHAPTER 3

ARTIFICIAL NEURAL NETWORK MODELS

3.1 Basic concepts and operating principles of artificial neural networks

As one branch of artificial intelligence, the theory of artificial neural networks was first introduced in the middle of the 20th century and numerous advances have been made since then. Researchers from many scientific disciplines are designing artificial neural networks to solve various problems like pattern recognition, optimization, control, forecasting and prediction, etc. In this section, important concepts and facts related to artificial neural networks have been briefly reviewed.

Before using ANN, it is essential to know what a neural network is. A neural network is a powerful data modeling tool designed on the basis of the human brain. It resembles the human brain in that it acquires knowledge through learning. This acquired knowledge is stored within inter-neuron connection strengths known as synaptic weights. The advantage of neural network is its ability to represent both linear and non-linear mathematical relationships and learn these relationships directly from given data. A neuron is the basic building block of a neural network.

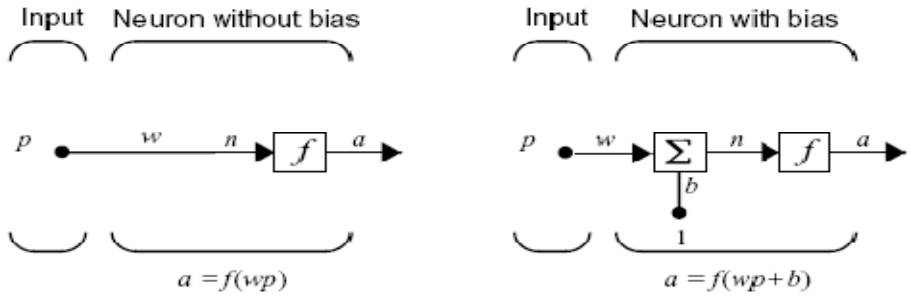

Fig.3.1: A neuron with and without bias

Fig. 3.1 shows a simple neuron. It consists of an input signal p, which is connected to a transfer function f via a synaptic space signified by w. The output of the network is given by a (output). (Deepak, 2008).

In a neuron with bias, the input b is connected directly to the transfer function f. Thus in this case, the whole input is presented by wp+b. The input signals like p are connected to a neuron via adjustable weights w. b signifies the variable bias of a neuron. Thus when a network is trained, these biases and weights keep on getting automatically adjusted as the training goes on. On the completion of training, these networks can predict on the basis of these adjusted weights and biases.. The result produced by a neural network on training is due to the transfer functions used. Following are the transfer functions generally used in a neural network.

1. Hard-limit transfer function.
2. Linear transfer function.
3. Tan-sigmoid transfer function.
4. Log-sigmoid transfer function

A perceptron neuron, which uses the hard-limit transfer function, is shown below. It has R no. of input signals.

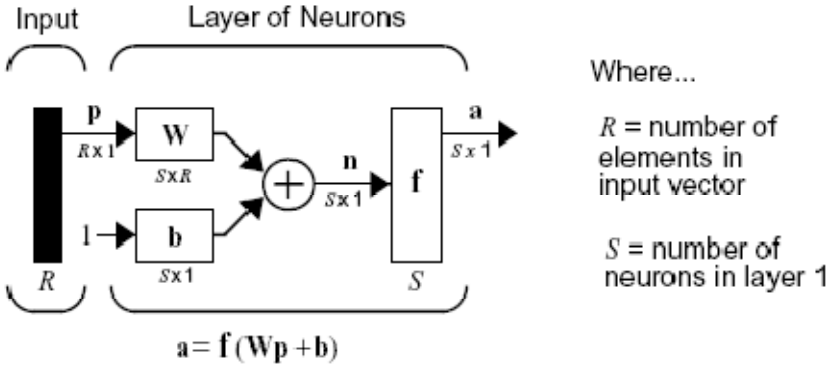

Fig.3.2: A Perceptron.

3.2 Computational models of neuron

Neurons processes input and produce output. Each neuron takes in the output from many other neurons. Once inside the neuron, the weighted signals are summed to a net value. In most models, they are simply added together. But in some cases the weights may have a negative value. Thus, when added in with excitatory signals they reduce to the overall signal input.

The equation below is basic to all neural networks:

$$\text{Net}_i = \sum_{j=1}^{p}(wij \times xj) \tag{3.1}$$

The equation means the net value for neuron i, net_i, equals the sum of input signal with the weights for all the inputs to the neuron i from neuron j starting at output of neuron j = 1 and ending at j = p. More simply, it means adding up all of the signals that are coming into this neuron, taking the connection strengths of each signal into account.

After finding the weighted sum of its inputs (net_i), the neuron calculates its output by applying an activation function. The activation function produces an activation level (a_i) inside the neuron. The neuron calculates its output by finding the weighted sum of its inputs (net_i) and then applying an activation function, which produces an activation level (a_i) inside the neuron. The activation is passed a transfer function f_i, which produces the actual output for that neuron for that time, $y_i(t)$.

In the simplest models, the activation function is the weighted sum of the neuron's inputs; the previous state is not taken into account. In more complicated models, the activation function also uses the previous output value of the neuron, so that the neuron can self-excite. These activation functions slowly decay over time; an excited state slowly returns to an inactive level. Sometimes the activation function is stochastic, i.e. it includes a random noise factor (Tao xie, 2004).

The state of activation is a way to refer to the state of the neural network at a given time. Each neuron has an individual activation value which can be written as $a_i(t)$, where a means activation, i is the neuron and (t) is a particular time. The activation function specifies what the neuron is to do with the signals after the weights have had their effect. The activation function could even be used to do some sort of time integration of the inputs, so that the neuron and the network exhibit time dependent behaviour.

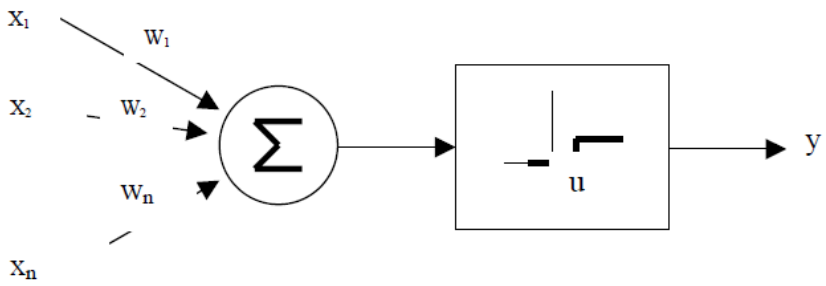

Fig.3.3: McCulloch pitts model. (Xie, 2004)

The activation is passed through a transfer function, which produces the actual output for that neuron. The transfer function of a neuron defines how the activation value is output. McCulloch and Pitts (1943) proposed a binary threshold unit as the transfer function. Their model is shown in Fig.3.3. For simplicity of notation, the threshold u can be considered as another weight w_o and be attached to the sum with a constant input $x_o = 1$.

McCulloch and Pitts (1943) proved that, in principle, suitably chosen weights let a synchronous arrangement of such neurons perform universal computation. This model contains a number of simplifying assumptions, however, that do not reflect the true behaviour of biological neurons (Xie, 2004).

The McCulloch and Pitts neuron has been generalized in many ways. One of them is to use a transfer function other than the threshold function, such as piecewise linear, sigmoidal, or

Gaussian, as shown in fig.3.4. The most common is the sigmoid function. It is a strictly increasing function that exhibits smoothness and has the desired asymptotic properties. The standard form is the logistic function, defined by

$$f(x) = 1/(1+\exp\{-\beta x\}) \qquad (3.2)$$

where β is the slope parameter

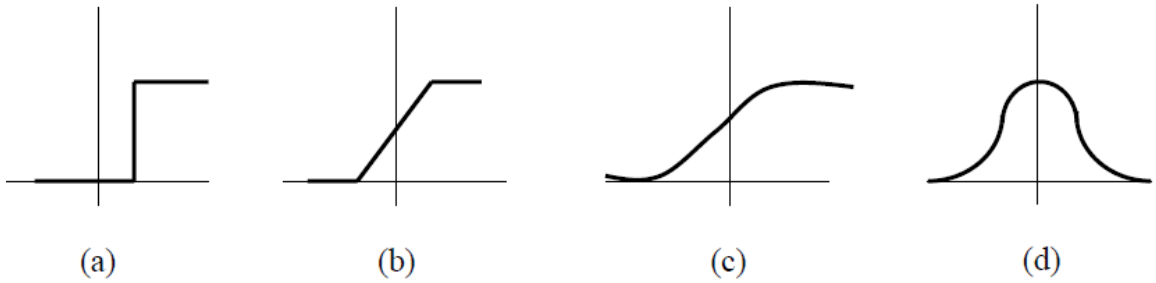

Fig.3.4: Different types of transfer functions: (a) threshold, (b) piecewise linear, (c) sigmoidal, and (d) Gaussian.

The sigmoid function is a particularly useful nonlinear transfer function. The sigmoid function has a high and a low saturation limit, and a proportional range in between. This function usually produces a 0 when the activation value is a large negative number and a 1 when the activation value is a large positive number, and makes a smooth transition in between. The sigmoid transfer function produces an output from –1 to +1 in some networks (Matlab-7 Help File)

Regardless of the exact transfer function, a neuron fires when it recognizes a particular value combination of incoming signals. In other words, neuron determines a match between the input vector, consisting of incoming signals, and a weight vector of internal parameter set.

3.3 Neural network architecture

Artificial neural networks can be viewed as weighted and directed graphs in which artificial neurons are nodes and directed edges (with weights) are connections between neuron outputs and neuron inputs (Jain et al., 1996). Based on their connection patterns, neural networks can be grouped into two categories:

• Feed-forward networks, in which no loop exists,

• Feedback (recurrent) networks, in which loops occur because of feedback connections.

Feed forward networks are less often considered to be associative memories than the feedback networks, although they can provide exactly the same functionality.

Nowadays, the most commonly used neural networks are nonlinear feed-forward models. The capacity of feedback networks has not thus far proved to be very impressive. In running mode, feed forward models are also faster, since they only need to make one pass through the system to find a solution.

Feed forward neural networks can be supervised or unsupervised. A supervised network compares its answers during training to known correct answers, whereas and unsupervised network (self-organizing) does not.

Different network architectures require different learning algorithms. The next section will discuss the most common learning processes (Xie, 2004)

3.4 Learning algorithms

The most attractive characteristics of artificial neural networks is their ability to mathematically learn by examples and repetitions. There are basically two learning paradigms: supervised learning and unsupervised learning. During supervised learning training, it requires *knowledge* of what the result should be. Output neurons are told what the ideal response to input signals should

be. For one-layer networks in which the stimulus-response relation can be controlled closely, this is easily accomplished by monitoring each neuron individually. In multi-layer networks, supervised learning is more difficult. Correction of hidden neuron layers is difficult. On the other hand, unsupervised learning does not have specific corrections made by an observer.

In the supervised learning, there exists a “teacher” or “trainer”, which may be implemented in various ways. Pairs of inputs and outputs are presented to the network. The network takes each input, produces an output and it then compares to the correct output. The trainer causes the network to construct an internal representation that captures the regularities of the data in a distributed and generalized way. This is the form of learning is presently most suitable to real applications.

In unsupervised learning, no “teacher” is involved. Instead, the network is simply exposed to a number of inputs. The network organizes itself in such a way as to come up with its own classifications for inputs (Xie, 2004)

3.5 Feed forward network

A number of perceptrons connected together as in fig.3.5 form a single layer of feedforward network.

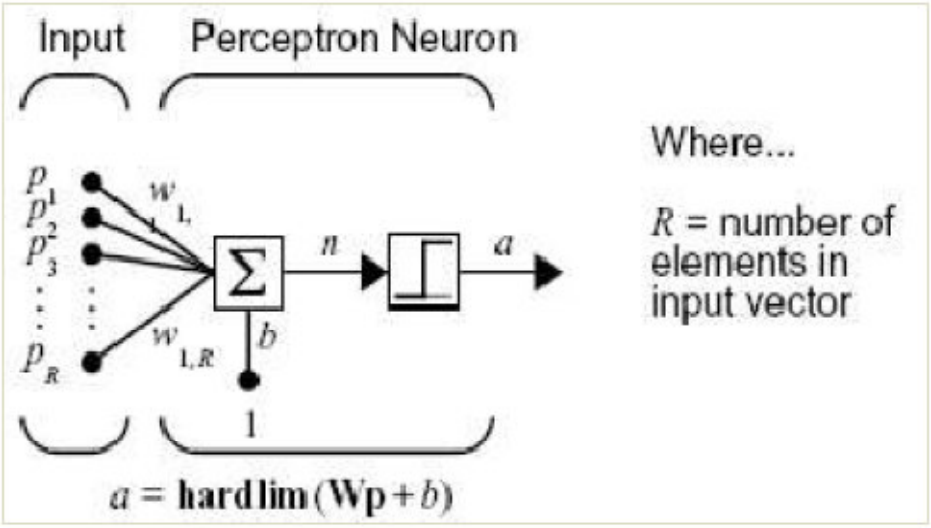

Fig.3.5: Feed forward network with perceptrons.

Here R input signals are connected to S number of neurons, each via its own weight. This is the example of a single layer of feed-forward network. A feed-forward network can have more than one layer as shown in fig.8. In that case, the last layer consists of only linear transfer functions and is known as output layer. All other layers are known as hidden layers. The number of neurons in each hidden layer, as well as the number of hidden layers has a profound effect on the output of a feed-forward network (Matlab-7 Help File).

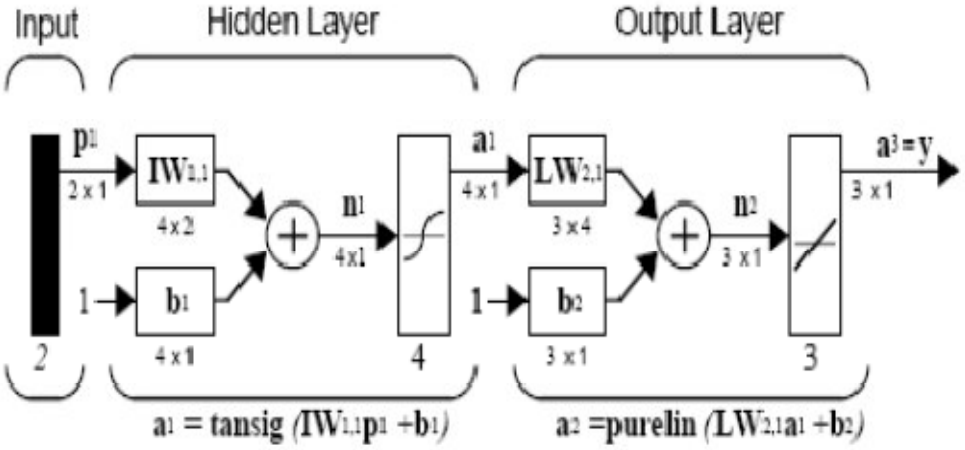

Fig.3.6: Multilayer feed forward network.

There are 3 steps in designing a feed-forward network:

1. Creating a network.

2. Training a network.

3. Simulating a network.

For training a network using back-propagation algorithm the commonly used inbuilt MATLAB-7 functions are trainlm, traingd, traingda and trainrp. There is also different performance parameters used while training a network using MATLAB-7 simulator like epochs, show, goal, time, min grad etc. Even though a number of techniques have been present for network topology selection, it still remains an iterative trial and error procedure.

3.6 Limitations of ANNs

Although artificial neural networks are very powerful tools for dealing with complex problems, they are not cure-all. Artificial neural networks heavily rely on their training samples. If the training samples are insufficient or do not cover all the typical conditions of the problem, errors can be large with testing samples. If the training samples are too much, they can also cause the over-fitting problem. The most important limitation of ANNs is that they do not reveal the exact nature of the relationship between inputs and outputs; in other words, the ANN models are hard to interpret or convert to rules. Besides, confidence intervals for predictions are not always available. Multiple models can be created from the same training data, as the nonlinear multivariable optimization for weight and biases is a "hard problem" with no guarantee of finding the global optimum. Interrupted training can be criticized as a method that depends on the optimization algorithm (only used with back-propagation). Regularization of weights relates to "maximum margin classifiers" but introduces one more tunable parameter. Due to

compounding nonlinearity, furthermore, the model behavior could be erratic in localized regions of the multidimensional input space (Xie, 2004).

CHAPTER-4

BED VOIDAGE

CHAPTER 4

BED VOIDAGE

The bed voidage or bed porosity is defined as the fraction of the bed volume occupied by both liquid and gas phases and as such directly proportional to the expanded bed height. The bed voidage is a strong function of liquid velocity but a weak function of gas velocity. The bed voidage is calculated using different correlations for different ranges of the variables and the data generated is fed as input to the multi-layer ANN. The architecture of multi-layer ANNs generally involves many layers each representing a set of parallel processing nodes. In theory a single hidden layer is sufficient for ANNs to approximate any complex nonlinear function, and experiments also confirm that one hidden layer suffices for most prediction problems. Fig. 4.1 shows a feed-forward ANN with one hidden layer as employed in this study. By successively adopting its own output to input layer, this ANN model can be used for the prediction of bed voidage.

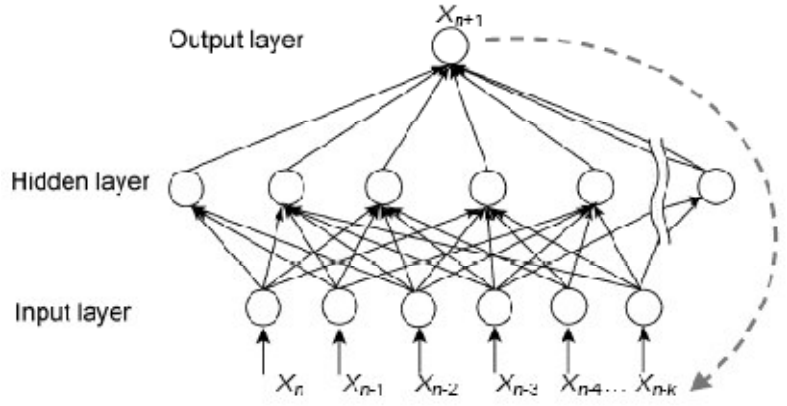

Fig.4.1: Multilayer neural network

4.1 Neural network model for bed voidage:

The correlations used for generating data of bed voidage as given in Appendix-I are:

[1]. Jean and Fan et al. correlation, 1986.

[2]. Han et al. correlation, 1990.

[3] Dakshinamurthy et al. correlation, 1972.

[4] Song et al. correlation, 1989.

For modeling the bed voidage the variables fed as input to the networks are Froude no. of gas, Reynold's no. of liquid, gas phase capillary group, modified Weber no. and the ratio of superficial liquid velocity and and terminal liquid velocity. Thus there are 5 inputs and the output is bed voidage. Both TRAINGDA and TRAINRP network algorithm were used for training. The performance results of the various network architectures used and the corresponding simulation results are given in tables 4.1, 4.2, 4.3, 4.4, 4.5, 4.6 below. Fig.4.2 shows that the optimum no. of nodes is 13. It is based on the least mean square error. The fig.4.3 and 4.5 give the performance graphs for the optimum no. of hidden neurons. In fig.4.4 the variation of bed voidage with Froude no. of gas is shown for various correlations calculated and the neural network output. Fig.4.6 gives the variation of bed voidage with the ratio of superficial liquid velocity and the terminal liquid velocity for various correlation and the ANN model predicted values.

Network configurations:

Table 4.1: Network configuration using TRAINGDA function for training

Network type	Transfer function	Learning function	No.of layers
Feed-forward backdrop	TRAINGDA	LEARNGDM	3

Table 4.2: Training performance using TRAINGDA function.

Data Source	No. of data	Epochs	Optimum No. of neurons in hidden layer	Mean squared error
[1],[2],[3],[4]	1650	1000	13	9.49×10^{-3}

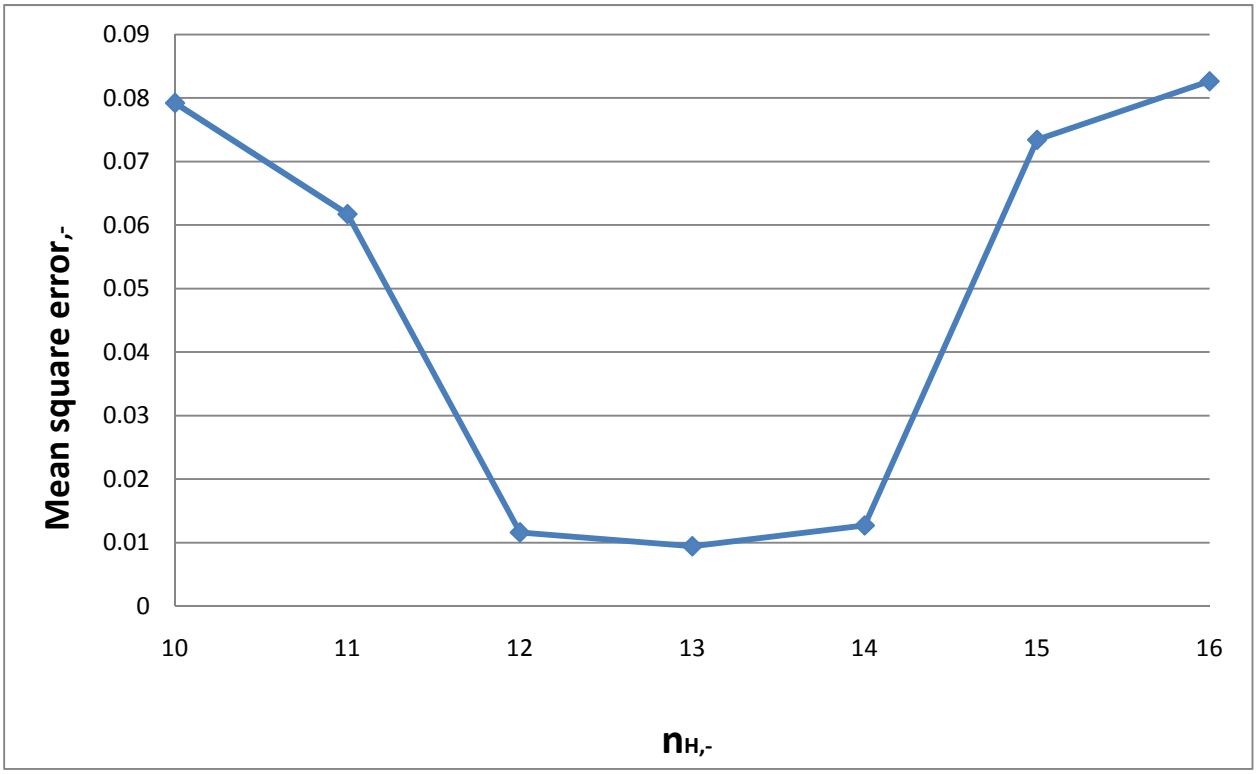

Fig.4.2: Plot of the variation of mean squared error with the no. of neurons in hidden layer.

Table 4.3: Simulation results for bed voidage.

Data source	No. of data	AAD (%)
[2]	100	17.10
[1]	100	12.30
[3]	100	15.53
[4]	100	18.90

$$\text{AAD}\ (\%) = \frac{1}{N} \times \sum_n \left(\frac{x_{predicted} - x_{calculated}}{x_{calculated}}\right) \times 100$$

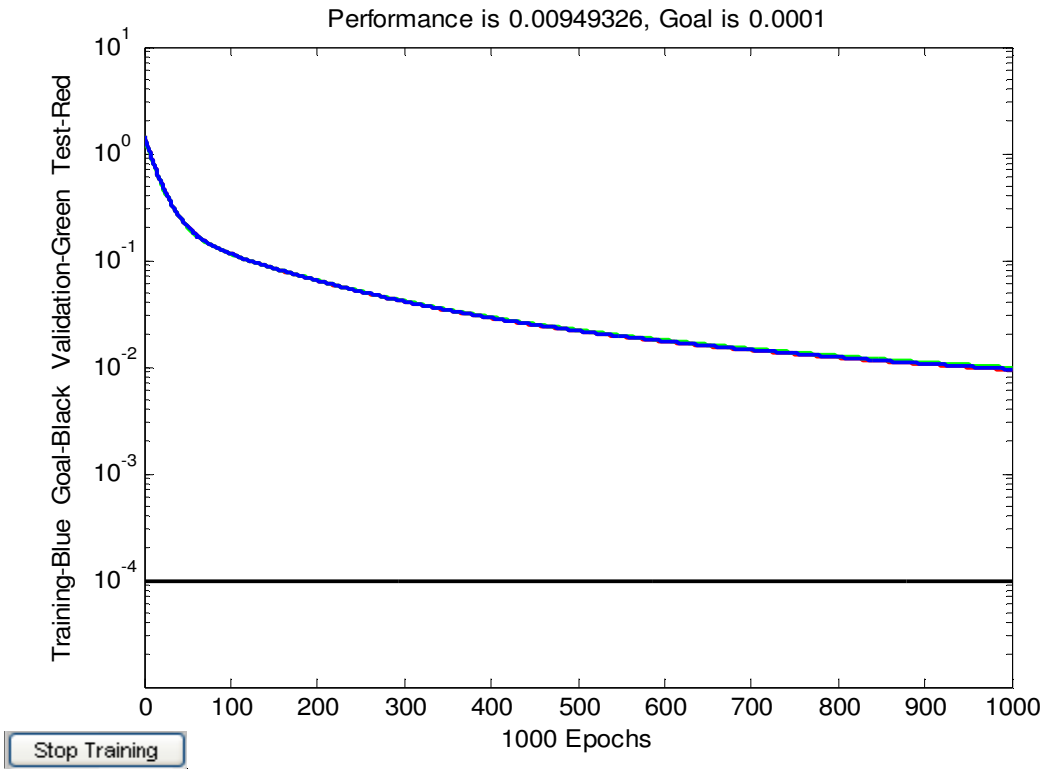

Fig.4.3: Training performance graph using TRAINGDA function

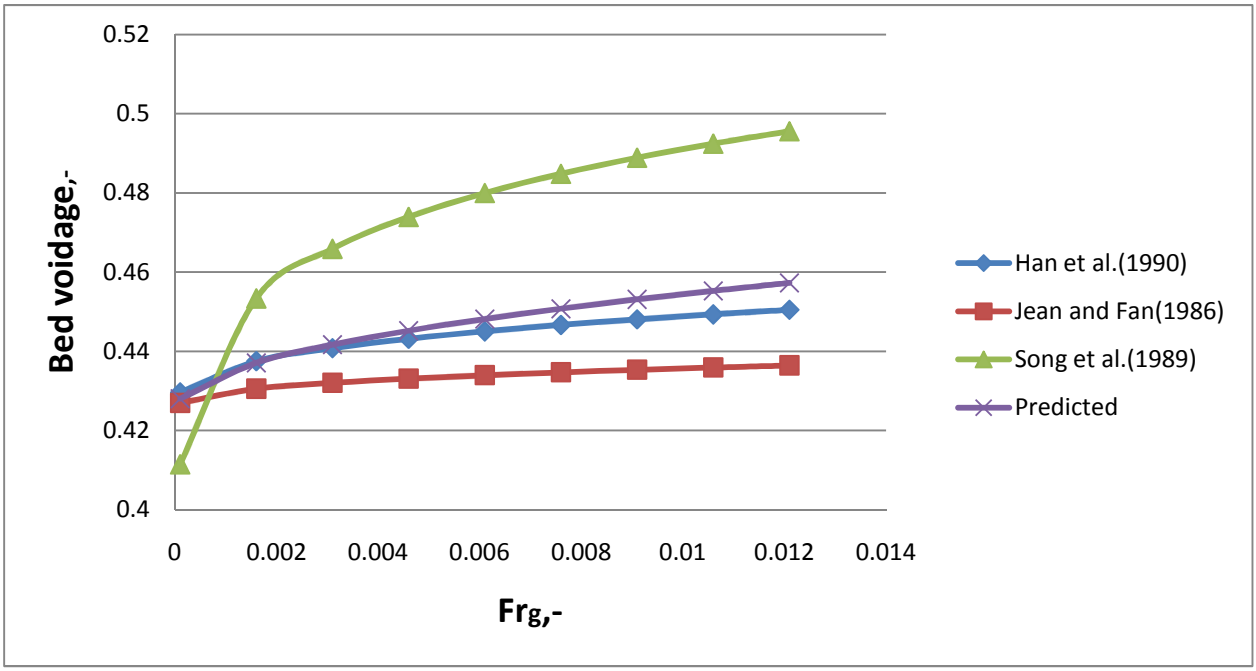

Fig.4.4: Plot of bed voidage vs. Froude no. of gas for various correlations calculated and ANN predicted values.

Table 4.4 : Network configuration using TRAINRP function for training.

Network type	Transfer function	Learning function	No.of layers
Feed-forward backdrop	TRAINRP	LEARNGDM	3

Table 4.5: Training performance using TRAINRP function.

Data source	No. of data	Epochs	Optimum No. of neurons in hidden layer	Mean squared error
[1],[2],[3],[4]	1200	1000	9	1.12×10^{-4}

Table 4.6: Simulation results for bed voidage.

Data source	No. of data	AAD (%)
[2]	100	1.36
[1]	100	6.78
[3]	100	5.97
[4]	100	2.105

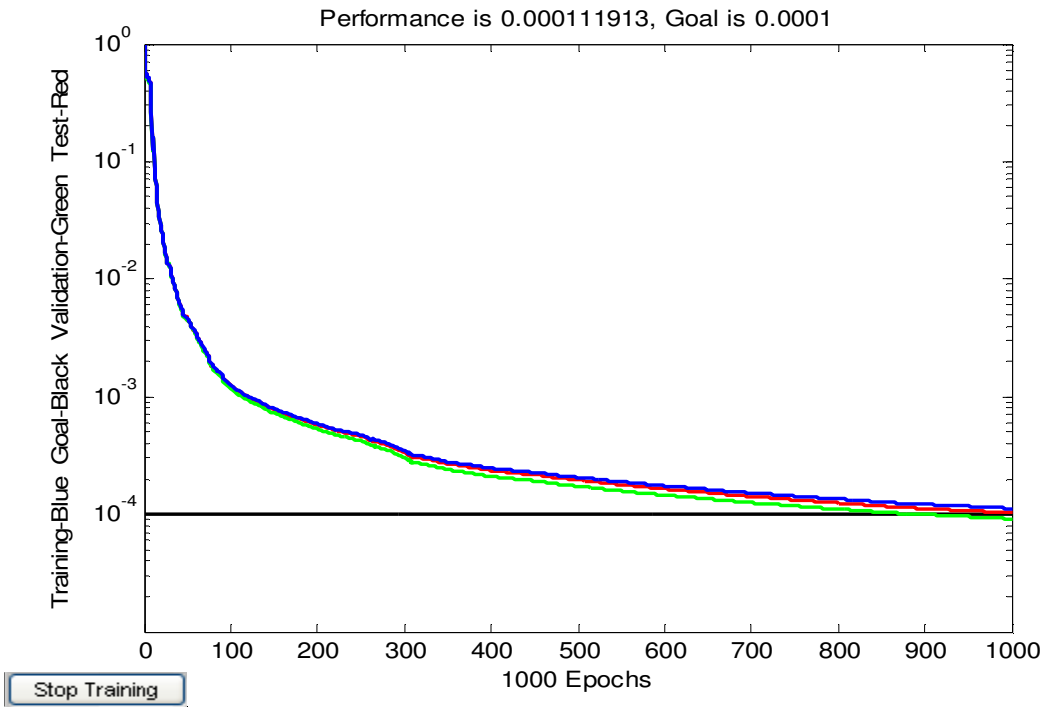

Fig.4.5: Training performance using TRAINRP function

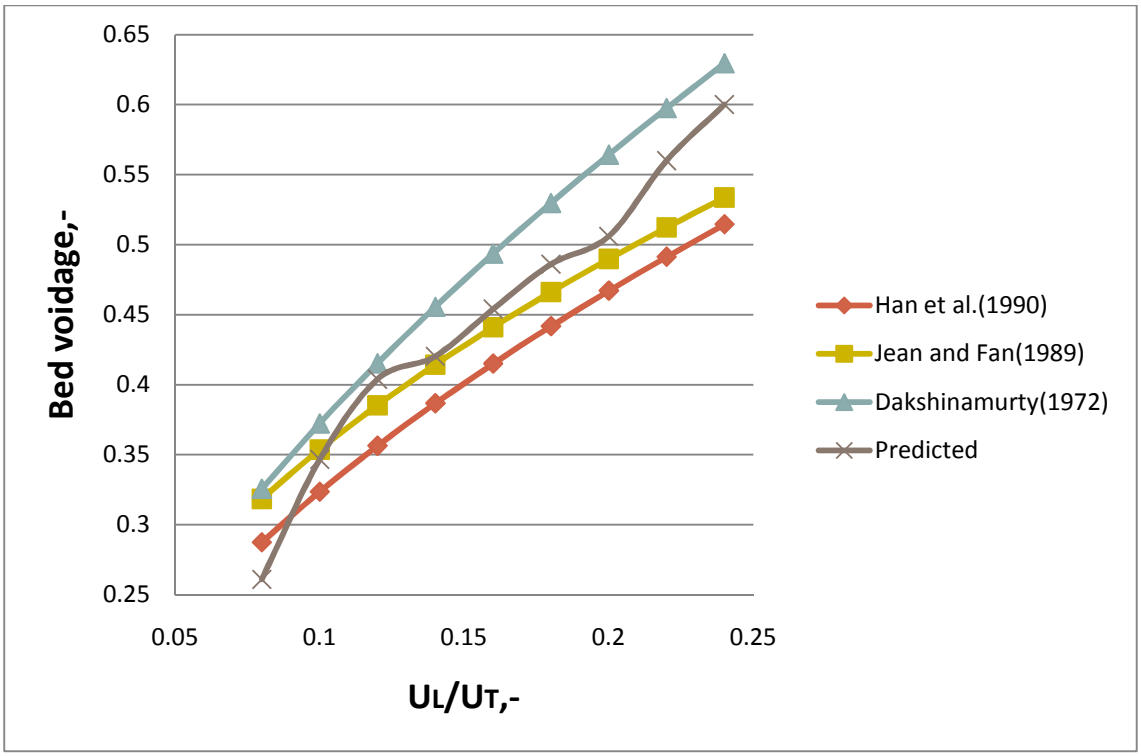

Fig.4.6: Plot of bed voidage vs. (U_l/U_t) for various correlations calculated and ANN predicted values.

4.2 Results and discussion

From the various networks the TRAINRP network gives a better performance with a greater accuracy (AAD<6.78%). The optimum no. of nodes in the hidden layer was 10 and 9 for the respective networks. The plots of various correlations show that the neural networks have been successfully able to predict the bed voidage for the random set of data.

CHAPTER-5

GAS HOLDUP

CHAPTER 5

GAS HOLDUP

The gas holdup is one of the most important characteristics for analyzing the performance of a three-phase fluidized bed. For chemical processes, where mass transfer is the rate-limiting step, it is important to be able to estimate the gas holdup since this relates directly to the rate of mass transfer .Gas holdup measures the fractional volume occupied by the gas. The variables which affect the gas holdup in fluidization are static bed height, particle size, liquid and gas velocity, orifice diameter, density of gas, liquid and solid, viscosity of gas and liquid, surface tension of liquid and the gravitational constant. These variables are varied in the valid ranges of the correlations and the data generated is used for training, validation and testing the performance of the ANNs. The trained ANNs are then used for simulating the hydrodynamic parameters to get the output for a random data set.

5.1 Neural network model of gas holdup:

For training the data consists of 1946 data points generated from various literature correlations. Various network configurations using TRAINLM function and TRAINRP function are given in the tables below. This helps in comparing between them which network design is better in predicting the holdup for the new data. The numbers of neurons in the hidden layer were varied and the effect on the performance of the ANN was observed. The correlations used for generating data of gas holdup as given in Appendix-I are:

[1]. Begovitch and Watson correlation, 1978.

[2]. Song et al. correlation, 1989.

[3]. Safoniuk et al correlation, 2002.

[4]. Jena et al correlation, 2009.

For modeling the gas holdup the variables fed as input to the networks are Froude no. of gas, Reynolds no. of liquid, Reynolds no. of gas and the Eotvos no. Thus there are 4 inputs and the output is gas holdup. The performance results of the various network architectures used and the corresponding simulation results are given in tables 5.1, 5.2, 5.3, 5.4, 5.5, 5.6 below. The fig.5.1 and 5.3 give the performance graphs. Fig. 5.2 gives the variation of gas holdup and Reynolds no. of liquid for various correlations calculated and that predicted by ANN model. It shows that the ANN model has generalized the relation to a good extent. Fig.5.4 gives the variation of gas holdup with Froude no. of gas for various correlations calculated and that predicted by ANN model.

Network configurations:

Table 5.1: Network configuration using TRAINGDA function for training.

Network type	Transfer function	Learning function	No.of layers
Feed-forward backdrop	TRAINGDA	LEARNGDM	3

Table 5.2: Training performance using TRAINGDA function.

Data source	No. of data	Epochs	Optimum No. of neurons in hidden layer	Mean squared error
[1],[2],[3],[4]	1946	500	11	3.30×10^{-2}

Table 5.3: Simulation results for gas holdup.

Data source	No. of data	AAD (%)
[2]	150	21.57
[4]	150	20.75
[3]	150	17.91
[1]	150	19.02

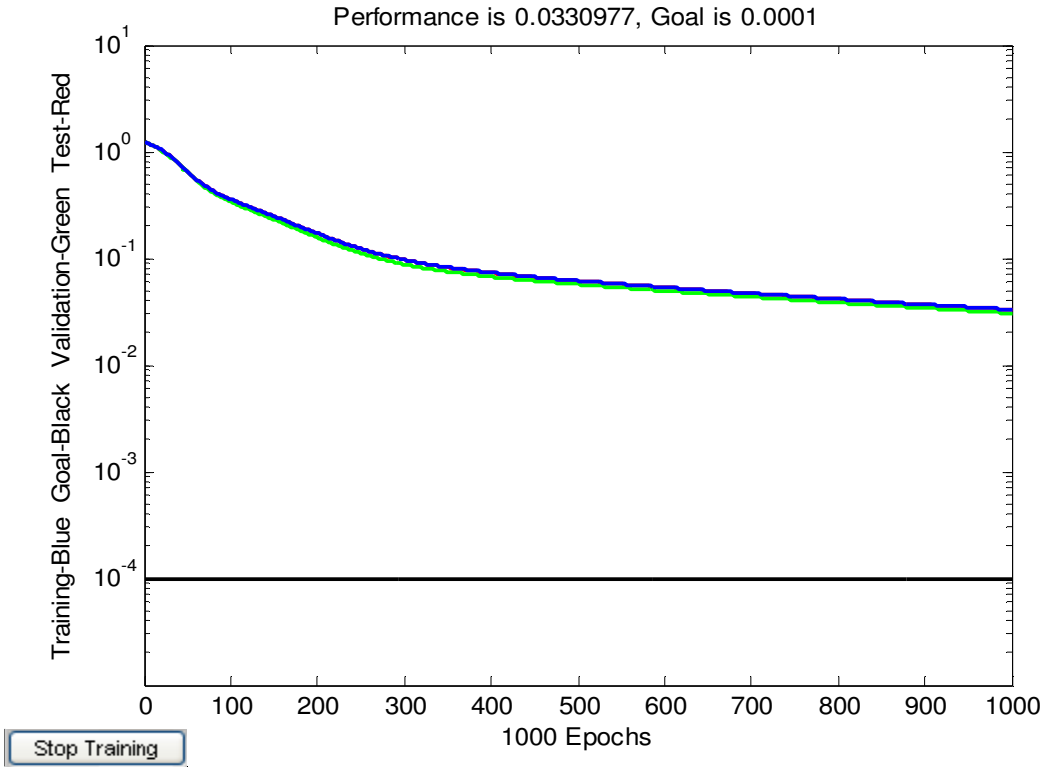

Fig.5.1: Training performance graph using TRAINGDA function

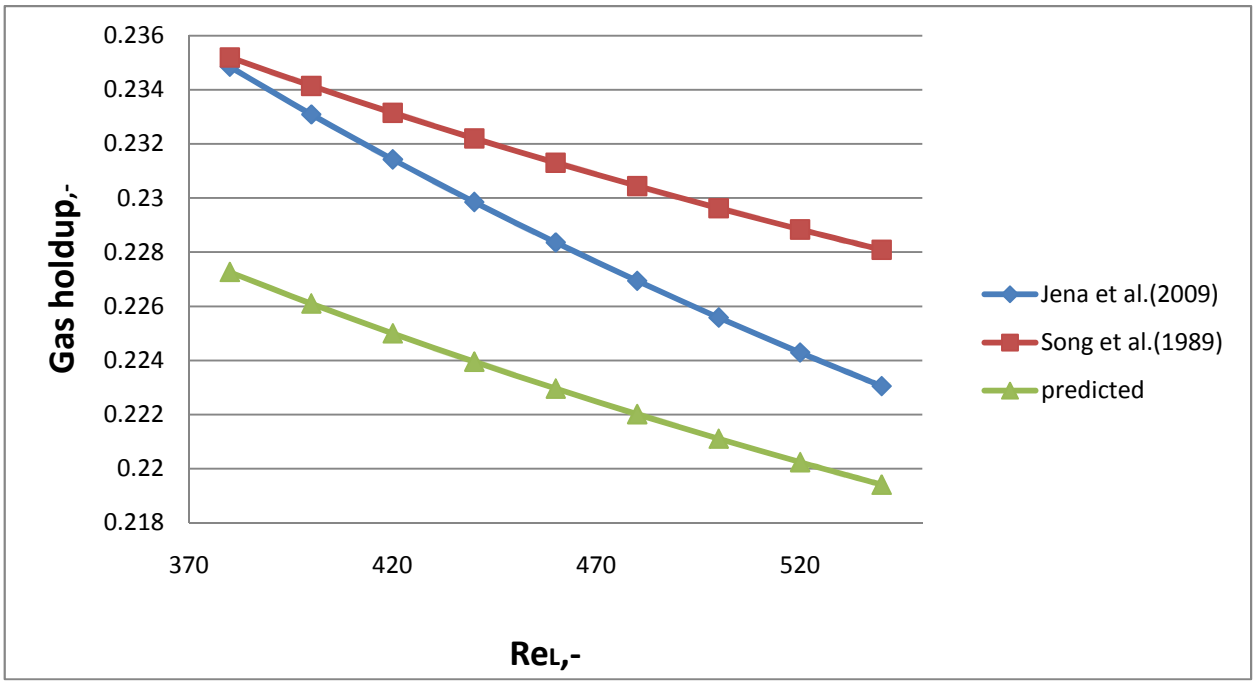

Fig.5.2: Plot of gas holdup vs. Reynolds no. of liquid for various correlations calculated and ANN predicted values.

Table 5.4: Network configuration using TRAIRP function for training

Network type	Transfer function	Learning function	No. of layers
Feed-forward backdrop	TRAINRP	LEARNGDM	3

Table 5.5: Training performance using TRAINRP function

Data source	No. of data	epochs	Optimum no. of neurons in hidden layer	Mean squared error
[1],[2],[3],[4]	1946	500	9	1.2×10^{-4}

Table 5.6: Simulation results for gas holdup

Data source	No. of data	AAD (%)
[2]	150	3.42
[4]	150	6.16
[3]	150	9.96
[1]	150	9.67

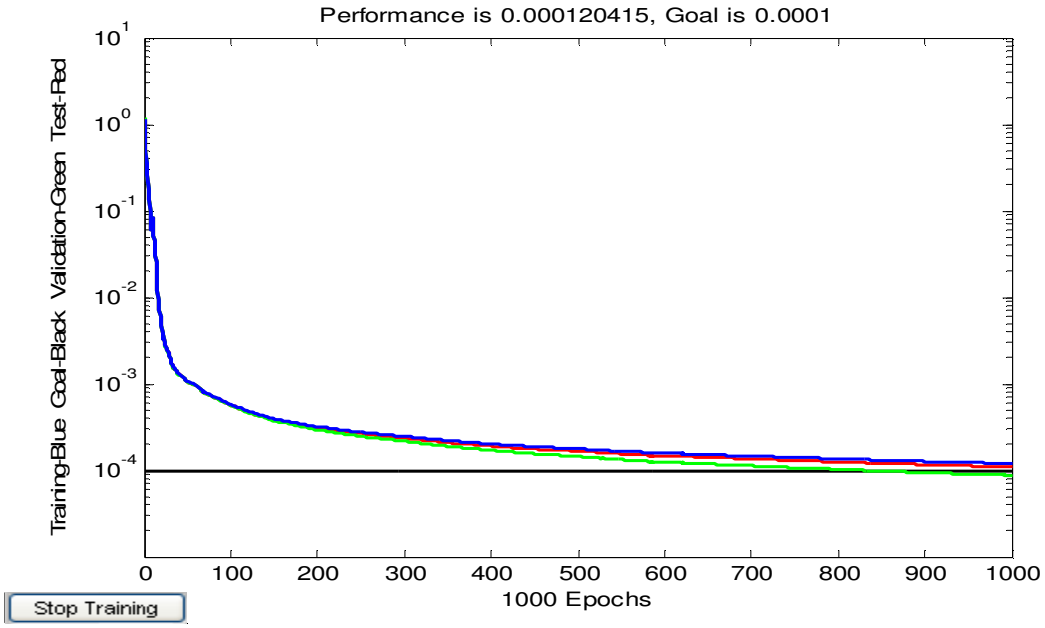

Fig.5.3: Training performance using TRAINRP function

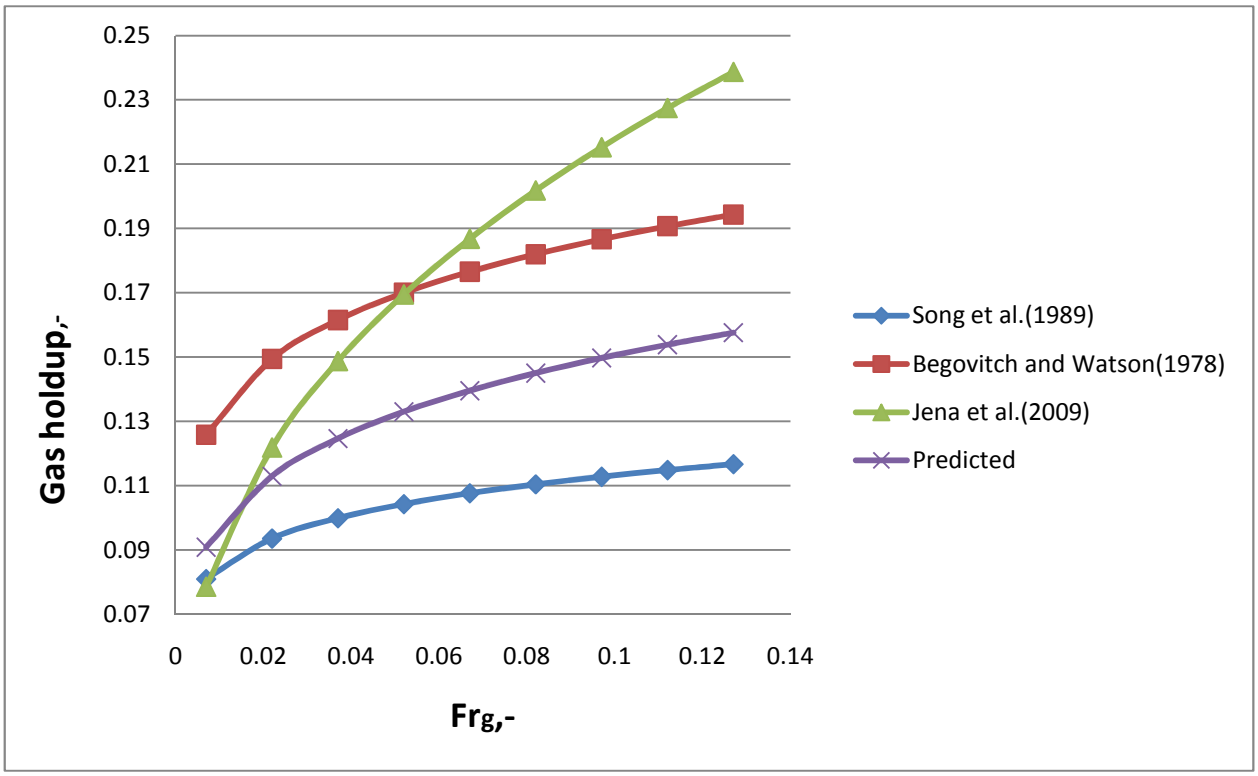

Fig.5.4: Plot of gas holdup vs. Froude no. of gas for various correlations calculated and ANN predicted.

5.2 Results and discussion

From the various networks the TRAINRP network gives a better performance with a greater accuracy (AAD<9.96%). The optimum no. of nodes in the hidden layer was 11 and 9 for the respective networks. The comparison plots of various correlations calculated and the ANN predicted values show a reasonably good prediction trend of the neural network.

CHAPTER-6

LIQUID HOLDUP

CHAPTER 6

LIQUID HOLDUP

Liquid holdup in three phase fluidization measures the amount of liquid in the bed. The factors affecting liquid holdup in the bed are the superficial liquid velocity, terminal liquid velocity, superficial gas velocity, density of liquid, diameter of column, surface tension of liquid and acceleration due to gravity. Various correlations are used to calculate the liquid holdup in the specific ranges of these variables. The data thus generated is fed as input to different ANNs. TRAINGDA and TRAINLM functions are used for training the networks. The goal for mean squared error is set at 0. Both feed forward backdrop and radial basis networks are used for training the networks. The no. of neurons in the hidden layer is varied for the 3 layer neural networks and the effect on mean squared error is investigated. The optimum no. of nodes (neurons) is selected based on the least mean squared error.

6.1 Neural network model of liquid holdup:

The correlations used for calculating liquid holdup as given in Appendix-I are:

[1]. Han et al. correlation, 1990.

[2]. Kato et al. correlation, 1985.

[3]. Kim et al. correlation, 1975.

For modeling the gas holdup the variables fed as input to the networks are Froude no. of gas, Froude no of liquid, modified Weber no. , Reynolds no. of liquid and the ratio of the superficial liquid velocity and the terminal liquid velocity. Thus there are 5 inputs and the output is liquid holdup. The performance results of the various network architectures used and the corresponding simulation results are given in tables 6.1, 6.2, 6.3, 6.4, 6.5 and 6.6 below. The fig. 6.1 and 6.3

give the performance graphs and the fig. 6.2 and 6.4 give the comparison plots of the network output and the values calculated from correlations for liquid holdup.

Network configurations for liquid holdup:

Table 6.1: Network configuration using TRAINGDA function for training.

Network type	Transfer function	Learning function	No. of layers
Feed-forward backdrop	TRAINGDA	LEARNGDM	3

Table 6.2: Training performance using TRAINGDA function.

Data source	No. of data	Epochs	Optimum No. of neurons in hidden layer	Mean squared error
[1],[2],[3],	1600	1000	11	4.12×10^{-3}

Table 6.3: Simulation results for liquid holdup.

Data source	No. of data	AAD (%)
[2]	200	20.46
[3]	200	18.91
[1]	200	22.31
[3]	200	17.71

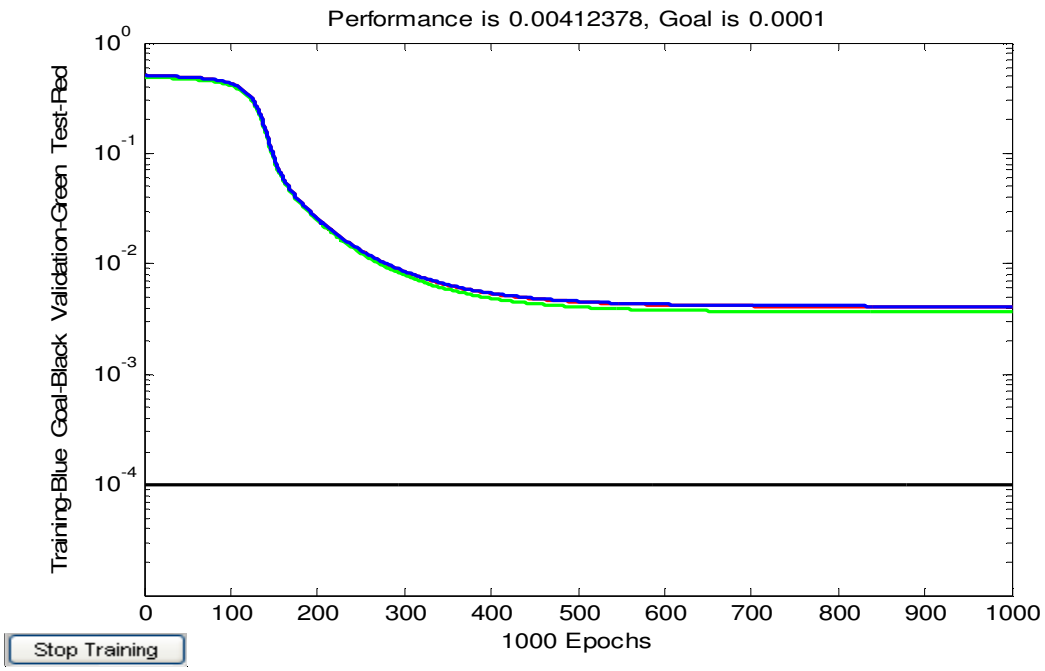

Fig.6.1: Training performance using TRAINGDA function

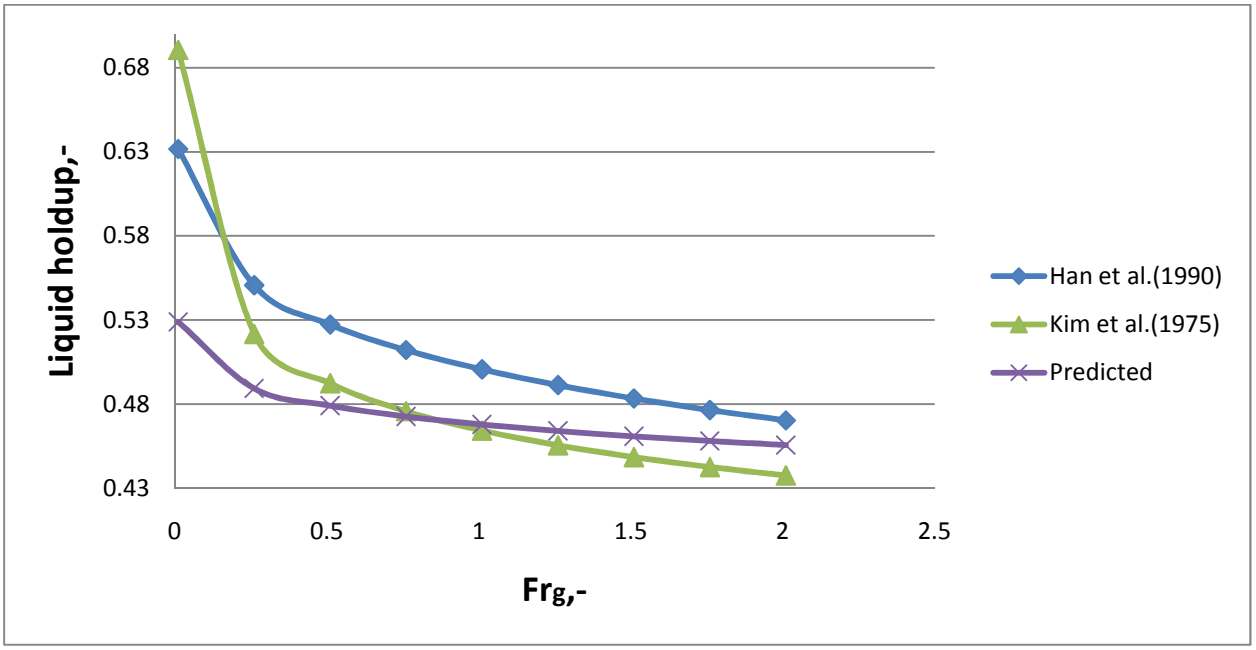

Fig.6.2: Plot of liquid holdup vs Froude no. of gas for various correlations calculated and ANN predicted values.

Table 6.4: Network configuration using TRAINRP function for training.

Network type	Transfer function	Learning function	No.of layers
Feed-forward backdrop	TRAINRP	LEARNGDM	3

Table 6.5: Training performance using TRAINRP function.

Data source	No. of data	Epochs	Optimum No. of neurons in hidden layer	Mean squared error
[1],[2],[3],	1600	1000	10	1.77×10^{-4}

Table 6.6: Simulation results for liquid holdup.

Data source	No. of data	AAD (%)
[2]	100	6.76
[1]	100	6.46
[1]	100	9.92
[3]	100	10.56

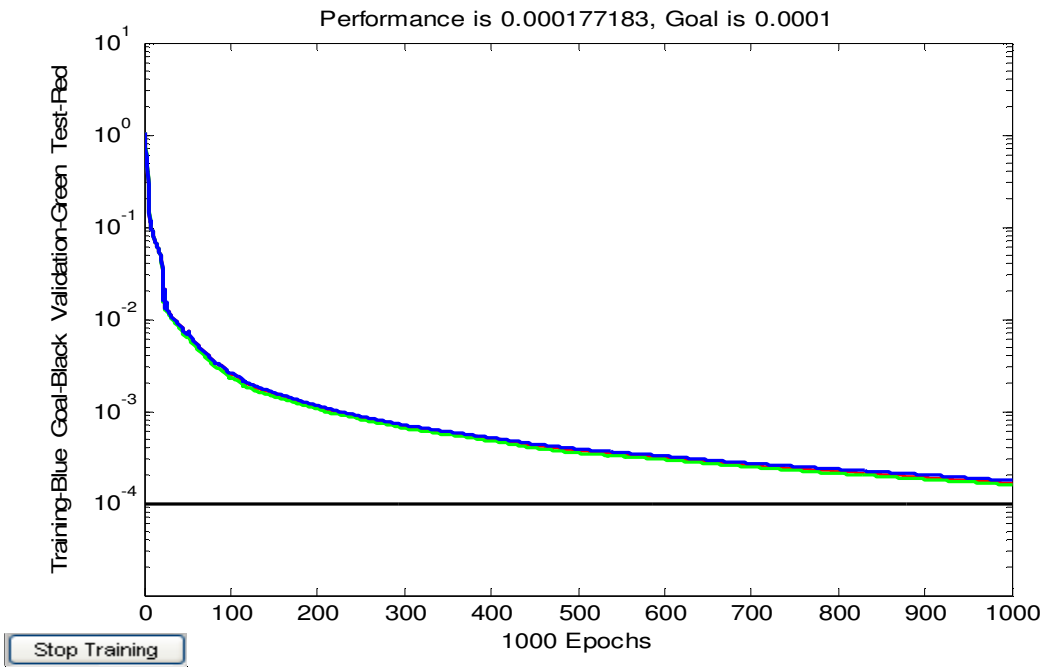

Fig.6.3: Training performance using TRAINRP function

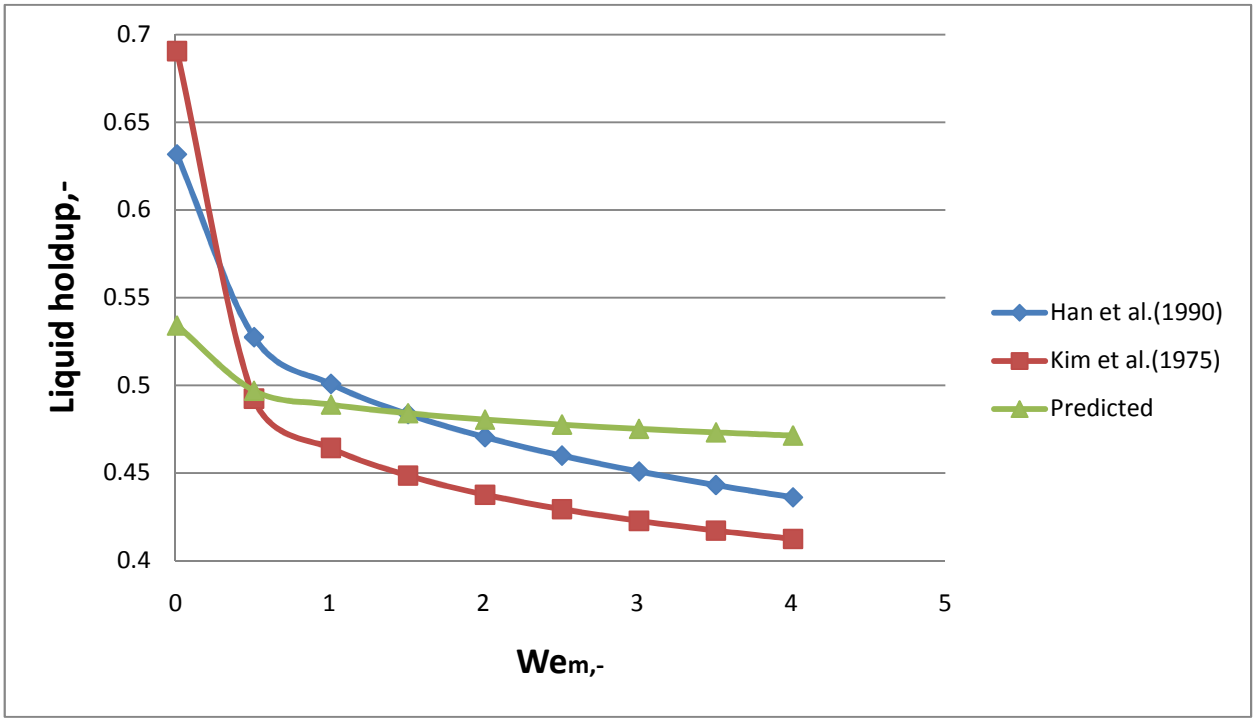

Fig.6.4: Plot of liquid holdup vs. Froude no. of gas for correlation calculated and ANN predicted values.

6.2 Results and discussion

From the various networks the TRAINRP network gives a better performance with a greater accuracy (AAD<.10.56%). The optimum no. of nodes in the hidden layer were 11 AND 10 respectively. The comparison plots also give a good generalization of the liquid holdup variation with different parameters. The graphs show that the neural networks were very accurate in predicting the gas holdup for the set of data.

CHAPTER-7

CONCLUSION

CHAPTER 7

CONCLUSION AND FUTURE SCOPE OF THE WORK

Neural networks are computer algorithms inspired by the way information is processed in the nervous system. The most important property of neural networks is the ability to learn. This learning property of neural networks helps in giving solutions when explicit algorithms and models are not available. In the present case the nonlinear variations of hydrodynamic characteristics have been modeled.

An artificial neural network model has been developed for modeling the hydrodynamic characteristics of the bed. The data has been generated using various literature correlations and various neural network architectures have been tested for generalizing the output. For the training of ANNs, the feed-forward backdrop algorithm has been used with the early stop training approach. The effects of the number of nodes in hidden layers on the training behavior of ANNs have been investigated. The training algorithm using TRAINRP transfer function produced a better performance than the TRAINGDA transfer function.

From the errors calculated it can be concluded that the neural networks have been successful in predicting the hydrodynamic parameters to a reasonable accuracy. For bed voidage the calculated AAD (%) has been less than 18.90%. for gas holdup and liquid holdup the corresponding AADs(%) calculated have been less than 21.57% and 22.31% respectively. When compared with the selected literature correlations, the ANN correlation shows noticeable agreement in the prediction of overall gas holdup.

Such ANN-based models can crucially assist in understanding the hydrodynamic nature of the fluidized bed. They hold high potential application to improve real-time monitoring, dynamic control and scale-up of fluidized beds. For practical applications, further work is undergoing to incorporate operating conditions into the model and try to use some artificial data as the initial input of the model.

REFRENCES

REFERENCES

Amit,K.,2009.CFD Modeling of Gas-Liquid-Solid Fluidized Bed. B.Tech Thesis, NIT-Rourkela,India.

Bhatia .V.K and Epstein.N, 1974. Three-phase fluidization: a generalized wake model , In: H. Angelino, J.P. Couderc, H. Gibert and H. Lagueric, Editors, Proceedings of the International Symposium on Fluidization, Its Application. Cepadues-Editions, Toulouse. 380–392.

Begovich, J.M., Watson, J.S., 1978. Hydrodynamic characteristics of three-phase fluidized beds. In "Fluidization". J.F. Davison and D.L. Keairns (Eds.), Cambridge University Press, Cambridge, 190-195.

Bloxom, V. R.; Costa, J. M.; Herranz, J.; MacWilliam, G. L.; Roth, S. R. 1975.Determination and Correlation of Hydrodynamic Variables in a Three-phase Fluidized Bed. Part IV,ORNL/MIT 219, Oak Ridge National Laboratory, Oak Ridge, TN.

Burghardta,A., Bartelmusa,G., Janeckib,D., Szlemp,A,2002. Hydrodynamics of a three-phase fixed-bed reactor operating in the pulsing flow regime at an elevated pressure. Chem. Eng. Sci. 57,4855 – 4863.

Dakshinamurty, P., Subrahmanyam, V., Rao, J. N. 1971. Bed Porosities in Gas-liquid Fluidization. Ind. Eng. Chem., Process Des. Dev.10, 322-328.

Dakshinamurty, P., Rao, J. N.. Subburaju K. V., Subrahmanyam, V., Rao, J. N., 1972. Bed Porosities in Gas-liquid Fluidization. Ind. Eng. Chem., Process Des. Dev., 11, 318-319.

Fan. L. S, 1989. Gas–Liquid–Solid Fluidization Engineering, Butterworth Series in Chemical Engineering; Butterworth: Stoneham, MA.

Han, J.H., Wild, G., Kim, S.D., 1990. Phase Hold-Up Characteristics in Three- Phase Fluidized Beds. Chem Eng J., 43. 67–73.

Jain, A. K., Mao, J., and Mohiuddin, K. M. 1996. Artificial neural networks: a tutorial. IEEE Computer, 31-44.

Jean, R.H., Fan, L.S., 1986. A Simple Correlation for Solids Holdup in a Gas- Liquid-Solid Fluidized Bed. Chem. Eng. Sci. 41. 2823-2828.

Jena,H.M., Sahoo,B.K., Roy,G.K., Meikap,B.C., 2008. Characterization of hydrodynamic properties of a gas–liquid–solid three-phase fluidized bed with regular shape spherical glass bead particles. Chem. Eng. J. 145. 50–56.

Jena,H.M., 2009. Hydrodynamics of Gas-Liquid-Solid Fluidized and Semi-Fluidized Beds. PhD Thesis, NIT-Rourkela, India.

Kato, Y.; Uchida, K.; Mooroka, S.; Kago, T.; Saruwatari, T.; Yang, S.-Z. 1985. Axial Holdup Distributions of Gas and Solid Particles in Three-phase Fluidized Bed for Gas-liquid (slurry)-solid Systems. J. Chem. Eng. Jpn, 18, 308-313.

Kim, S. D., Baker, C. G. J., Bergougnou. M. A 1975. Phase Holdup Characteristics of Three-phase Fluidized Beds. Can. J. Chem. Eng, 53, 134-139.

Larachi, F.,Belfares, L., Iliuta, I., Grandjean, B.P.A., 2001. Three-phase Fluidization Macroscopic Hydrodynamics Revisited". Ind. Eng. Chemistry and Research, 40 993-1008.

Lee, S.L.P., de Lasa, H.I., 1987. Phase holdups in three-phase fluidised beds. AIChE J, 33 1359–1370.

Luo X., Jiang P., Fan L.S. 1997. High-pressure three-phase fluidization: hydrodynamics and heat transfer, AIChE. J, 43. 2432–2445.

Rout.D.R., 2008. Application of ANN in predicting VLE data of CO2-Aqueous-Alkanolamine System. B.Tech Thesis, NIT-Rourkela,India.

Safoniuk, M., Grace, J.R., Hackman, L., McKnight, C.A., 2002. Gas Hold-Up in a Three-Phase Fluidized Bed. AIChE J. 48, 1581-1587.

Song, G.H., Bavarian, F., Fan, L.S., 1989. Hydrodynamics of three-phase fluidized bed containing cylindrical hydrotreating catalysts. Can. J. of Chem. Eng. 67, 265-275.

Xie.T, 2004. Hydrodynamic characteristics of gas/liquid /fibre three phase flows based on objective and minimally-intrusive pressure fluctuation measurements. PhD Thesis, Georgia institute of Technology.

APPENDIX-I

Table 8: Correlations used for data generation.

Researcher	**Correlations**	**System(Gas/liquid/ solids)**
[1]. Jean and Fan et al. correlation, 1986.	$\varepsilon = (U_L/U_t)^{0.56}(1 + 0.123Fr^{0.347}We_m^{0.037})$	Air/viscous solutions /glass beads
[2].Han et al. correlation, 1990.	$\varepsilon = (U_L/U_t)^{0.60}(1 + 0.123Fr^{0.347}Re_L^{0.1166})$	Air /aqueous solutions of glycerol/glass beads
[3]Dakshinamurthy et al. correlation, 1972.	$\varepsilon = 2.65(U_L/U_t)^{0.6}(Ca_g)^{0.08}$	Air/water/glass beads and lead shot; nitrogen/ electrolyte/glass beads and Rockwool shot
[5]. Begovitch and Watson correlation, 1978.	$\varepsilon_g = 0.159\ (Fr_g)^{0.15}(Eo)^{0.13}$	Air/water/glass beads
[6]. Song et al. correlation, 1989.	$\varepsilon_g = 0.280(Fr_g)^{0.126}(Re_L)^{-0.0873}$	Air/ aqueous t-pentanol solution /cylindrical particles
[7]. Safoniuk et al correlation, 2002.	$\varepsilon_g = 0.014(Re_g)^{0.426}$	Air/ tap water and aqueous glycerol solutions/aluminium cylinders
[8]. Jena et al correlation, 2009	$\varepsilon_g = 1.3567(Fr_g)^{.3835}(Re_L)^{-0.1466}$	Air/water/rasching rings
[9]. Han et al. correlation, 1990.	$\varepsilon_l = (U_L/U_t)^{0.65}(1 - .374Fr_g^{.176}We_m{}^{-0.173})$	Air/tapwater/glass beads
[10]. Kato et al. correlation, 1985.	$\varepsilon_l = (U_L/U_t)^{0.54}\ (1 - 9.7(350 + Re_L{}^{1.1}))^{-0.5}$	Air/water/ aqueous solutions of carboxy methyl cellulose(CMC), glass beads
[11]. Kim et al. correlation, 1975.	$\varepsilon_l = 1.504(Re_L)^{-0.082}(Fr_g)^{-0.086}(Fr_L)^{0.234}$ $(We_m)^{0.092}$	Air/ solutions of commercial grade sugar and CMC/glass beads and irregular gravel